

Cite this: *Chem. Sci.*, 2015, **6**, 3533Received 25th March 2015
Accepted 14th April 2015DOI: 10.1039/c5sc01083g
www.rsc.org/chemicalscience

Introduction

A variety of complex three-dimensional supramolecular architectures have been templated using non-coordinating anions bound in internal binding pockets.^{1–10} Such anions may be present either as the counterion of the metal salt, or added externally. The dynamic nature of host–guest complexes, which enables their formation, can facilitate subsequent structural rearrangements driven by replacement of one anion for another.^{11,12} Building upon these foundations, here we show that complex $M^{II}X_4^{2-}$ anions may serve as templates for intricate three-dimensional structures. These anions are constructed from the same dicationic first-row transition-metal ions that form the vertices of the host framework, and they are generated during the same equilibration process that generates the host. Their use as structural templates provides an added layer of complexity in the synthesis of metal–organic capsules.

Subcomponent self-assembly, where ligands and complex come together during the same overall process, has proven useful in the preparation of a variety of new materials^{13–20} and functional structures.^{21–28} We have previously reported its use in the preparation of a diverse range of discrete three-dimensional architectures^{29,30} starting with *p*-toluidine and 6,6'-diformyl-3,3'-bipyridine subcomponents, and cobalt(II) or zinc(II) salts (NO_3^- , BF_4^- , ClO_4^- or $CF_3SO_3^-$) as templates. In contrast, when cobalt(II) or zinc(II) bis(trifluoromethane)sulfonimide (triflimide, NTf_2^-) is employed, a dynamic library (DL) is observed because

Mutual stabilisation between $M^{II}L_6$ tetrahedra and $M^{II}X_4^{2-}$ metallate guests†

Imogen A. Riddell,‡ Tanya K. Ronson and Jonathan R. Nitschke*

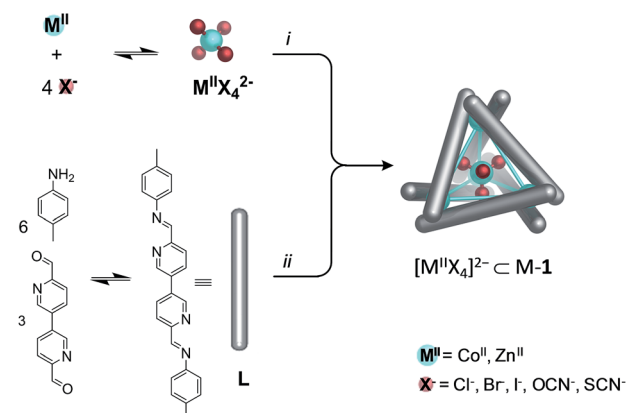
A complex host–guest equilibrium employing metal ions incorporated into both the host and guest is discussed. $M^{II}X_4^{2-}$ metallate guests are shown to provide a good size and shape match for encapsulation within the M_4L_6 tetrahedral capsules, facilitating the generation of previously unreported Zn_4L_6 complexes. Displacement of the initial, primary template anion ($ZnBr_4^{2-}$) by a secondary template anion (ClO_4^-) is shown to result in the formation of a pentagonal-prismatic $Zn_{10}L_{15}$ structure that incorporates both Br^- and ClO_4^- . Furthermore, the formation of heterometallic complexes provides direct evidence for metal exchange between the guest and host complex.

the triflimide anion is too large to serve as a template.³¹ Herein we discuss addition of halide or pseudohalide anions Cl^- , Br^- , I^- , OCN^- or SCN^- to $Zn(NTf_2)_2$ or $Co(NTf_2)_2$ -containing DL's. These reactions result in the *in situ* generation of complex metallate anions, which serve as optimal templates for M_4L_6 tetrahedra.^{32–34} Structural interconversion between a Zn_4L_6 tetrahedron, Zn-1, containing a centrally bound dianionic guest, and a larger $Zn_{10}L_{15}$ pentagonal architecture, Zn-2, templated by five monoanionic ClO_4^- anions was also demonstrated.

Results and discussion

Synthesis of $[MX_4]^{2-} \subset M_4L_6$ complexes

When the subcomponents of L (Scheme 1) were mixed with $Co^{II}(NTf_2)_2$ (6 equiv. L per 4 equiv. Co^{II}), a broad 1H NMR spectrum characteristic of a dynamic library of different



Scheme 1 Subcomponent self-assembly of $[MX_4]^{2-} \subset M_4L_6$ complexes showing both of the equilibration processes necessary for complex formation; (i) formation of the metallate template and; (ii) self-assembly of the ligand L.

Department of Chemistry, University of Cambridge, Lensfield Road, Cambridge, CB2 1EW, UK. E-mail: jrn34@cam.ac.uk

† Electronic supplementary information (ESI) available: Full experimental procedures, NMR, ESI-MS and UV-Vis spectra and details of the calculated void volumes and CIFS. CCDC 1047195–1047198. For ESI and crystallographic data in CIF or other electronic format see DOI: [10.1039/c5sc01083g](https://doi.org/10.1039/c5sc01083g)

‡ Current address: Massachusetts Institute of Technology, Department of Chemistry, 77 Massachusetts Avenue, Cambridge, MA 02139, USA.

coordination complexes (Co-DL) was observed. Following the addition of KBr (4 equiv. per 5 equiv. Co^{II}) to Co-DL, the ^1H NMR spectrum displayed a single sharp resonance per ligand proton environment (Fig. S1†). ESI-MS analysis provided evidence for a tetrabromocobaltate $[\text{Co}^{\text{II}}\text{Br}_4]^{2-}$ adduct of **1** (Fig. S2†). No evidence for a simple bromide adduct was obtained when less KBr was employed, suggesting that $[\text{Co}^{\text{II}}\text{Br}_4]^{2-}$ provides an optimal size, shape and Coulombic fit for the cavity of **1**.

Further evidence for formation of $[\text{Co}^{\text{II}}\text{Br}_4]^{2-}$ was obtained through UV-Vis spectroscopy, which displayed characteristic $[\text{Co}^{\text{II}}\text{Br}_4]^{2-}$ absorbance bands in the 500–800 nm window. The complex absorbance profile is indicative of the multiple accessible electronic excited states which are available to tetrahedral cobalt species,³⁵ and corresponds well to the absorbance of the $[\text{Co}^{\text{II}}\text{Br}_4]^{2-}$ dianion in the absence of the Co_4L_6 tetrahedral cage (Fig. S3†).

Unambiguous structural characterisation of the host–guest complex was obtained through single-crystal X-ray analysis (Fig. 1a and b). The structure of $[\text{CoBr}_4]^{2-} \subset \text{Co-1}$ was solved in cubic space group $F\bar{4}_132$ with one twelfth of the *T*-symmetric molecule in the asymmetric unit. The encapsulated $[\text{CoBr}_4]^{2-}$ anion thus occupies a special position of tetrahedral symmetry. Its Co–Br bond length of $2.424(1)$ Å is in good agreement with the average value of $2.40(2)$ Å found for $[\text{CoBr}_4]^{2-}$ anions reported in the Cambridge Structural Database.³⁶

A variety of other dianions were previously investigated as potential guest molecules for this metal–ligand system, however, no evidence was obtained for the formation of a host–guest complex upon addition of Na_2SO_4 , Na_2SeO_4 , Na_2TeO_4 , Na_2MoO_4 , $(\text{NH}_4)_2\text{SnF}_6$, or K_2CrO_4 .³¹ The increased energy of desolvation associated with dianions relative to their mono-anionic counterparts generally makes their encapsulation less energetically favourable.^{34,37–39} Thus $[\text{Co}^{\text{II}}\text{Br}_4]^{2-}$ is both the first dianionic guest to be bound within Co-1, and the largest guest to be accommodated within its cavity (Scheme 1).

The tight fit of $[\text{Co}^{\text{II}}\text{Br}_4]^{2-}$ within the tetrahedral host is apparent from Fig. 1b, as is the complimentary shape of the host–guest pair.³⁸ The centrally bound tetrahedral guest adopts a complementary orientation to that of the $\text{Co}^{\text{II}}_4\text{L}_6$ tetrahedron, wherein each bromide points directly out of an open face of the

capsule. In contrast, when the octahedral anion SbF_6^- was bound within Co-1, not all of the fluorine atoms can orient towards an open face of the tetrahedron (Fig. 1c). The shape match between $[\text{CoBr}_4]^{2-}$ and **1** thus facilitates accommodation of this large (115 Å 3) anion within Co-1. Further evidence of a good fit is provided by the observation that the Co–Co distances ($9.763(1)$ Å) of host **1** in $[\text{CoBr}_4]^{2-} \subset \text{Co-1}$ were not observed to lengthen from the $9.681(3)$ – $9.825(3)$ Å and $9.753(3)$ – $9.863(3)$ Å Co–Co distances observed for the SbF_6^- and MeCN⁴⁰ inclusion complexes, respectively. This observation indicates that the increased size of the dianionic template does not affect the size of the central binding pocket, leading us to hypothesise that other tetrahedral species, which have longer arms that are capable of protruding through the faces of the capsule,^{41–43} might prove suitable templates for Co-1.

Our hypothesis was tested using the pseudohalide OCN^- , which displays similar reactivity to Br^- , and is known to generate the $[\text{Co}^{\text{II}}(\text{OCN})_4]^{2-}$ dianion.^{44,45} The addition of KOCN (0.4 equiv.) to Co-DL followed by sonication and heating at 323 K for 24 hours yielded a ^1H NMR profile consistent with the formation of a tetrahedral capsule. The broad ^1H NMR profile associated with the mixture of species present in the Co-DL simplified to show one set of resonances per ligand proton, as was observed with KBr. ESI-MS also confirmed formation of the $[\text{Co}^{\text{II}}(\text{OCN})_4]^{2-} \subset \text{Co-1}$ complex (Fig. S5†).

The ability to generate host–guest complexes such as $[\text{Co}^{\text{II}}(\text{OCN})_4]^{2-} \subset \text{Co-1}$, where the guest molecule occupies the centre of the capsule but extends through the open faces of the host expands the potential range of applications for these metal–organic cage molecules. Most importantly this property allows host–guest complexes to be generated using guest molecules that are larger than the volume of the internal binding pocket, a property that restricts potential application of these capsules.⁴³

In common with cobalt(II) complexes, zinc(II) complexes can be either four- or six-coordinate. Furthermore, no crystal field stabilisation effects are observed for zinc(II) complexes due to their d^{10} electronic configuration, implying that a wider range of ligands might be employed to generate the tetrahalozincate

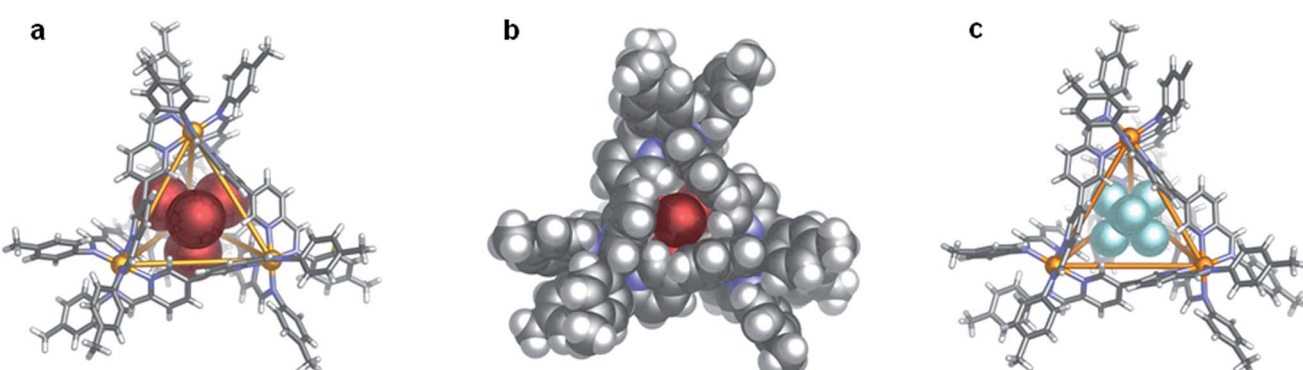


Fig. 1 Single-crystal X-ray structures of Co_4L_6 tetrahedra; (a) $[\text{CoBr}_4]^{2-} \subset \text{Co-1}$, stick representation of the host with the centrally bound anion shown in a space-filling representation and (b) host and guest both shown in space-filling mode, highlighting the tight fit of the guest within the symmetry-matched capsule; (c) $\text{SbF}_6^- \subset \text{Co-1}$. Solvent, counterions and disorder are omitted for clarity. Atom colours; carbon grey, hydrogen white, nitrogen blue, cobalt(II) orange, bromine red, fluorine cyan.



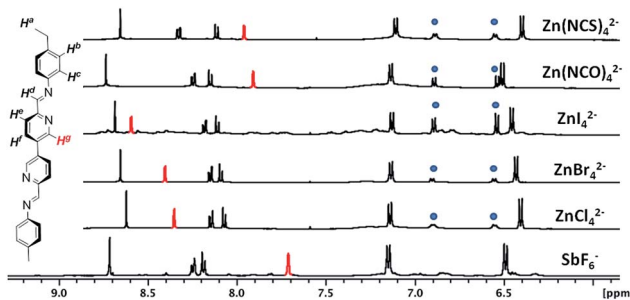


Fig. 2 ^1H NMR (400 MHz, 298 K, CD_3CN) of a range of Zn_4L_6 tetrahedra, **Zn-1**, with anionic guests; (a) SbF_6^- ; (b) $[\text{ZnCl}_4]^{2-}$; (c) $[\text{ZnBr}_4]^{2-}$; (d) $[\text{ZnI}_4]^{2-}$; (e) $[\text{Zn}(\text{NCO})_4]^{2-}$; (f) $[\text{Zn}(\text{NCS})_4]^{2-}$. Proton H^g indicated in red, experiences the greatest change in chemical shift with anion variation. Blue dots indicate excess *p*-toluidine.

inclusion complexes. The diamagnetic nature of this series of complexes also allows more subtle changes in the chemical environments of the host–guest complexes to be probed by ^1H NMR (Fig. 2).

As with Co^{II} , when a range of halide and pseudohalide anions were added directly to the **Zn-DL** generated from the subcomponents of **L** and $\text{Zn}(\text{NTf}_2)_2$, the complex ^1H NMR associated with the mixture of species in the dynamic library simplified to give a well defined ^1H NMR profile displaying one resonance per ligand proton, consistent with the formation of Zn_4L_6 tetrahedral complexes (Fig. 2). The ^1H NMR resonance corresponding to H^g (Fig. 2), which is directed across the open face of the Zn_4L_6 complexes, showed the greatest variation in chemical shift upon guest binding. For the series of halide anions, Cl^- , Br^- and I^- , a significant downfield shift of H^g relative to $\text{SbF}_6^- \subset \text{Zn-1}$ was observed. This observation is consistent with increasing contact between the larger centrally-bound anions and H^g . In contrast, the octahedral SbF_6^- anion cannot align itself effectively with the open faces of the tetrahedron and therefore does not effect a substantial change in the chemical shift of H^g .

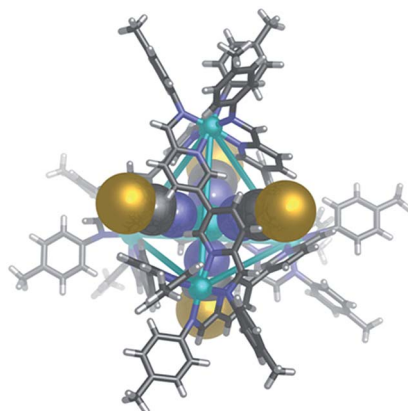


Fig. 3 Visualisation of template anion–ligand proton orientation for $[\text{Zn}(\text{NCS})_4]^{2-} \subset \text{Zn-1}$ and $[\text{Zn}(\text{NCO})_4]^{2-} \subset \text{Zn-1}$. Image based on the single crystal X-ray structure of $[\text{CoBr}_4]^{2-} \subset \text{Co-1}$, where the $[\text{CoBr}_4]^{2-}$ guest is replaced with $[\text{Zn}(\text{NCS})_4]^{2-}$. Atom colours: carbon grey, hydrogen white, nitrogen blue, zinc(II) turquoise, sulfur gold.

The ^1H NMR profiles of the host–guest complexes containing $[\text{Zn}(\text{NCO})_4]^{2-}$ and $[\text{Zn}(\text{NCS})_4]^{2-}$ reflect the longer protruding arms of these guest anions, compared with the metallate anions generated from the halide precursors. The H^g resonances for **Zn-1** encapsulating $[\text{Zn}(\text{NCO})_4]^{2-}$ and $[\text{Zn}(\text{NCS})_4]^{2-}$ are less downfield-shifted compared with those of the **Zn-1** complexes generated in the presence of Cl^- , Br^- and I^- . Furthermore, the 4,4'-bipyridine resonance, H^f , experiences a downfield shift which we attribute to interaction of this proton with the protruding isocyanato or isothiocyanato arm (Fig. 3). Formation of the isocyanato and isothiocyanato complex anions is expected to be preferred over the corresponding cyanato and thiocyanato isomers, in accordance with the position of these ligands in the spectrochemical series.⁴⁴

Dynamic rearrangement of $[\text{MX}_4]^{2-} \subset \text{M}_4\text{L}_6$ complexes

The observation that Br^- could induce formation of **1** when added to **Co-DL** is of interest for two reasons: firstly, the ability to selectively bind tetrahalometallate anions over their corresponding halide anions in organic media, particularly chloride, is of great interest in the hydrometallurgy industry.^{46–48} Secondly, Br^- binds within the centre of $\text{Co}^{II}{}_{10}\text{L}_{15}$ pentagonal prism, **Co-2**,⁴⁰ which self-assembles from *p*-toluidine, 6,6'-diformyl-3,3'-bipyridine and $\text{Co}^{II}(\text{ClO}_4)_2$ in acetonitrile.⁴⁰ Similarly, addition of KBr (0.6 equiv.) to the reaction mixture generated from *p*-toluidine, 6,6'-diformyl-3,3'-bipyridine and $\text{Zn}(\text{ClO}_4)_2$ generates a $\text{Zn}_{10}\text{L}_{15}$ complex with five peripherally bound ClO_4^- anions and a centrally bound bromide anion, $\text{Br}^- \subset \text{Zn-2}$. The single-crystal X-ray structure of $\text{Br}^- \subset \text{Zn-2}$ (Fig. 4) indicates that the complex is isostructural to previously reported $\text{M}_{10}\text{L}_{15}$ complexes formed from the same ligand,^{31,40} and to its chloride bound analogue (details of $\text{Cl}^- \subset \text{Zn-2}$ are provided in the ESI†).

No significant differences are observed in the size of the perchlorate-containing peripheral binding pockets of the

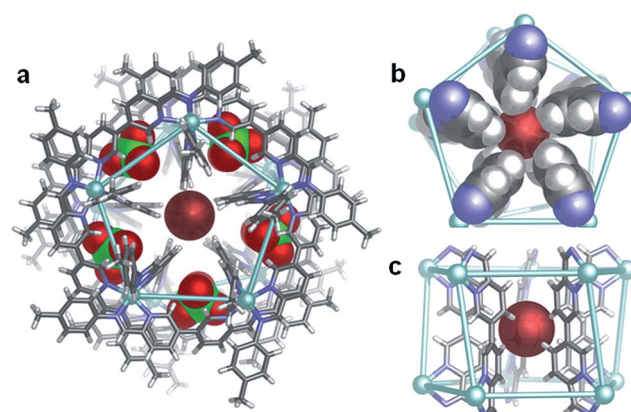
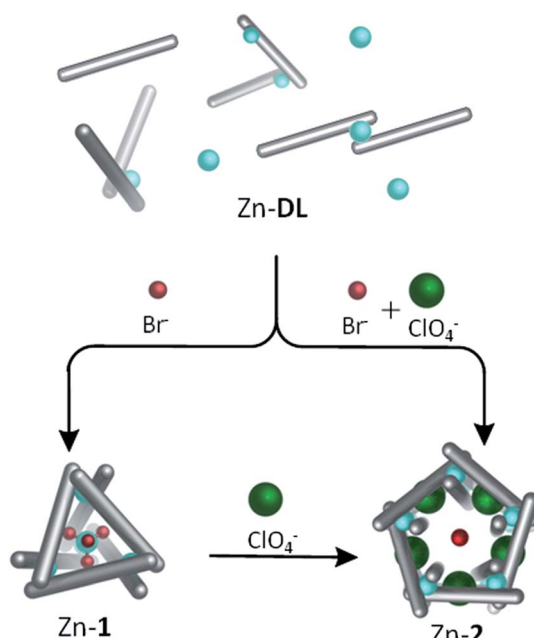


Fig. 4 Single-crystal X-ray structure of $\text{Br}^- \subset \text{Zn-2}$; (a) indicating the overall connectivity of the structure; (b) cut away view of the central binding pocket, highlighting the tight fit of the bromide anion within the central binding pocket; (c) side on view of the same complex showing that the bromide anion is bound at the centre of the channel through H-bonding with ten inward-pointing pyridyl hydrogen atoms. Disorder is omitted for clarity.





Scheme 2 Interconversion pathways between Zn-DL, Zn-1 and Zn-2. Zn-1 is generated from Zn-DL upon addition of bromide anions, which generate $[\text{ZnBr}_4]^{2-}$ metallate anions mutually stabilised upon encapsulation within the M_4L_6 tetrahedral host. Zn-2 can be generated from Zn-1 upon addition of ClO_4^- anions. Increasing the ratio of Br^- to ClO_4^- anions does not facilitate conversion of Zn-2 to Zn-1.

chloride and bromide adducts of Zn-2. Average void volumes of 83 \AA^3 and 82 \AA^3 for the perchlorate pockets of the Cl^- and Br^- complexes, respectively, were measured using VOIDOO.⁴⁹

Two reactions performed in parallel highlight the second-order templation effect⁴⁰ of the ClO_4^- anion within this system. Under identical conditions, KBr (0.6 equiv.) was added to two portions of Zn-DL, one of which contained LiClO_4 (0.8 equiv.). In the absence of perchlorate, the tetrabromozincate anion was generated and acted as a template for tetrahedron Zn-1. In the presence of perchlorate, however, the larger pentagonal prismatic structure, Zn-2, was formed with a single bromide anion bound at its centre, and no evidence for formation of Zn-1 was observed (Scheme 2). The different pathways followed by the system highlight its finely balanced thermodynamics, and the differential influence of the tetrabromozincate and perchlorate template anions. Increasing the salt concentration of the reaction mixture led to significant precipitation, but after addition of more than 1.3 equiv. of LiClO_4 , which is more than four times the amount required to template the $\text{M}_{10}\text{L}_{15}$ complex from Zn-DL, to a solution containing solely $[\text{ZnBr}_4]^{2-} \subset \text{Zn-1}$ the ratio of Zn-1 : Zn-2 was 1 : 8. In contrast, increasing the concentration of Br^- in the reaction mixture of $\text{Br}^- \subset \text{Zn-2}$ generated precipitate, and no evidence was obtained for formation of $[\text{ZnBr}_4]^{2-} \subset \text{Zn-1}$ in solution (Fig. S20†). These results indicate that the pentagonal prismatic structure Zn-2 is favoured over the tetrahedron, Zn-1, in the presence of both ClO_4^- and Br^- in solution.

For all of the reactions described herein, no evidence was obtained for association of the M_4L_6 complexes with either simple halide anions,^{50,51} or more than one dianion. ESI-MS of

each reaction mixture displayed peaks corresponding to $[\text{MX}_4]^{2-} \subset [\text{M}_4\text{L}_6]^{8+}$, where the remaining charge was in all cases balanced by triflimide counterions. The same results were obtained when the preformed anions $[\text{CoBr}_4]^{2-}$ and $[\text{CoCl}_4]^{2-}$ were added directly to Co-DL.

The self-assembly of heterometallic species was also investigated. ^1H NMR analysis of reaction mixtures generated from addition of $[\text{CoBr}_4]^{2-}$ or $[\text{CoCl}_4]^{2-}$ anions to Zn-DL indicated several paramagnetically shifted resonances clustered across distinct spectral regions. In contrast to the complex ^1H NMR, the ESI-MS spectra consisted of well-defined m/z peaks displaying an unusually wide distribution. Taken together these observations led us to postulate that a dynamic library of mixed metal species had been formed with overlapping m/z peaks (Fig. S21–26†). Observation of complexes containing multiple cobalt metal centres indicates that the $[\text{CoX}_4]^{2-}$ salts are a suitable source of cobalt(II) for generation of Co_4L_6 tetrahedra in the presence of solubilising counterions.

Conclusions

In conclusion, a family of novel $[\text{MX}_4]^{2-} \subset \text{M}_4\text{L}_6$ host–guest complexes has been identified, extending the limited range of M_4L_6 tetrahedral complexes known to encapsulate dianionic guests.^{21,52,53} These new $[\text{MX}_4]^{2-} \subset \text{M}_4\text{L}_6$ complexes readily self-assemble from complex dynamic libraries upon addition of a range of halide or pseudohalide anions. Self-assembly of both the host and the guest occurs during the same equilibration process, and neither the host nor guest was observed to be stable in the absence of the other under these conditions. Further investigations into the properties of these capsules indicated that association of more than one dianion per tetrahedral capsule is not favoured for solubility reasons, an observation previously made by Ward and co-workers.⁵² An unprecedented symbiosis was thus observed, in which cobalt(II) or zinc(II) exist in a dynamic equilibrium occupying roles either within a tetrahedral metallate guest or as an octahedral metal centre defining the vertices of the host framework. A clear hierarchy was observed in the stability of these structures, whereby the pentagonal prism Zn-2 was favoured over such tetrahedral structures as $[\text{ZnBr}_4]^{2-} \subset \text{Zn-1}$. These structures and their dynamic interconversions may have future roles to play in novel hydrometallurgical processes.^{46–48}

Acknowledgements

This work was supported by the U.K. Engineering and Physical Sciences Research Council (EPSRC). The authors thank W. J. Ramsay for calculation of tetrahalometallate anion volumes, and the Diamond Light Source (U.K.) for synchrotron beam time on I19 (MT7984 and MT8464).

Notes and references

- 1 H. T. Chifotides, I. D. Giles and K. R. Dunbar, *J. Am. Chem. Soc.*, 2013, **135**, 3039–3055.



2 H. T. Chifotides and K. R. Dunbar, *Acc. Chem. Res.*, 2013, **46**, 894–906.

3 C. S. Campos-Fernandez, B. L. Schottel, H. T. Chifotides, J. K. Bera, J. Bacsa, J. M. Koomen, D. H. Russell and K. R. Dunbar, *J. Am. Chem. Soc.*, 2005, **127**, 12909–12923.

4 C. Klein, C. Guetz, M. Bogner, F. Topic, K. Rissanen and A. Luetzen, *Angew. Chem., Int. Ed.*, 2014, **53**, 3739–3742.

5 M. D. Ward, *Chem. Commun.*, 2009, 4487–4499.

6 R. L. Paul, Z. R. Bell, J. C. Jeffery, J. A. McCleverty and M. D. Ward, *Proc. Natl. Acad. Sci. U. S. A.*, 2002, **99**, 4883–4888.

7 J. S. Fleming, K. L. V. Mann, C.-A. Carraz, E. Psillakis, J. C. Jeffery, J. A. McCleverty and M. D. Ward, *Angew. Chem., Int. Ed.*, 1998, **37**, 1279–1281.

8 Q.-Q. Wang, V. W. Day and K. Bowman-James, *Angew. Chem., Int. Ed.*, 2012, **51**, 2119–2123.

9 R. Custelcean, *Chem. Soc. Rev.*, 2014, **43**, 1813–1824.

10 R. Custelcean, in *Constitutional Dynamic Chemistry*, ed. M. Barboiu, Springer, Berlin Heidelberg, 2012, vol. 322, ch. 197, pp. 193–216.

11 W. Meng, T. K. Ronson, J. K. Clegg and J. R. Nitschke, *Angew. Chem., Int. Ed.*, 2013, **52**, 1017–1021.

12 M. Scherer, D. L. Caulder, D. W. Johnson and K. N. Raymond, *Angew. Chem., Int. Ed.*, 1999, **38**, 1587–1592.

13 X. Wu, N. Xu, Z. Zhu, Y. Cai, Y. Zhao and D. Wang, *Polym. Chem.*, 2014, **5**, 1202–1209.

14 X. Chen, N. Xu, N. Li, L. Lu, Y. Cai, Y. Zhao and D. Wang, *Soft Matter*, 2013, **9**, 1885–1894.

15 H. Bunzen, Nonappa, E. Kalenius, S. Hietala and E. Kolehmainen, *Chem.-Eur. J.*, 2013, **19**, 12978–12981.

16 K. S. Chichak, S. J. Cantrill, A. R. Pease, S.-H. Chiu, G. W. V. Cave, J. L. Atwood and J. F. Stoddart, *Science*, 2004, **304**, 1308–1312.

17 D. A. Leigh, P. J. Lusby, S. J. Teat, A. J. Wilson and J. K. Y. Wong, *Angew. Chem., Int. Ed.*, 2001, **113**, 1586–1591.

18 J.-F. Ayme, J. E. Beves, D. A. Leigh, R. T. McBurney, K. Rissanen and D. Schultz, *Nat. Chem.*, 2012, **4**, 15–20.

19 V. E. Campbell, R. Guillot, E. Riviere, P.-T. Brun, W. Wernsdorfer and T. Mallah, *Inorg. Chem.*, 2013, **52**, 5194–5200.

20 M. Mastalerz, H.-J. S. Hauswald and R. Stoll, *Chem. Commun.*, 2012, **48**, 130–132.

21 S. Yi, V. Brega, B. Captain and A. E. Kaifer, *Chem. Commun.*, 2012, **48**, 10295–10297.

22 K.-C. Sham, S.-M. Yiu and H.-L. Kwong, *Inorg. Chem.*, 2013, **52**, 5648–5650.

23 F. Reichel, J. K. Clegg, K. Gloe, K. Gloe, J. J. Weigand, J. K. Reynolds, C.-G. Li, J. R. Aldrich-Wright, C. J. Kepert, L. F. Lindoy, H.-C. Yao and F. Li, *Inorg. Chem.*, 2014, **53**, 688–690.

24 J. Roukala, J. Zhu, C. Giri, K. Rissanen, P. Lantto and V.-V. Telkki, *J. Am. Chem. Soc.*, 2015, **137**, 2464–2467.

25 X.-P. Zhou, J. Liu, S.-Z. Zhan, J.-R. Yang, D. Li, K.-M. Ng, R. W.-Y. Sun and C.-M. Che, *J. Am. Chem. Soc.*, 2012, **134**, 8042–8045.

26 J. Dömer, J. C. Slootweg, F. Hupka, K. Lammertsma and F. E. Hahn, *Angew. Chem., Int. Ed.*, 2010, **49**, 6430–6433.

27 P. D. Frischmann, V. Kunz, V. Stepanenko and F. Würthner, *Chem.-Eur. J.*, 2015, **21**, 2766–2769.

28 S. E. Howson, A. Bolhuis, V. Brabec, G. J. Clarkson, J. Malina, A. Rodger and P. Scott, *Nat. Chem.*, 2012, **4**, 31–36.

29 P. Mal, D. Schultz, K. Beyeh, K. Rissanen and J. R. Nitschke, *Angew. Chem., Int. Ed.*, 2008, **47**, 8297–8301.

30 W. J. Ramsay, T. K. Ronson, J. K. Clegg and J. R. Nitschke, *Angew. Chem., Int. Ed.*, 2013, **52**, 13439–13443.

31 I. A. Riddell, Y. R. Hristova, J. K. Clegg, C. S. Wood, B. Breiner and J. R. Nitschke, *J. Am. Chem. Soc.*, 2013, **135**, 2723–2733.

32 J. R. Nitschke, *Angew. Chem., Int. Ed.*, 2004, **43**, 3073–3075.

33 Z. Rodriguez-Docampo, E. Eugenieva-Ilieva, C. Reyheller, A. M. Belenguer, S. Kubik and S. Otto, *Chem. Commun.*, 2011, **47**, 9798–9800.

34 Z. Rodriguez-Docampo, S. I. Pascu, S. Kubik and S. Otto, *J. Am. Chem. Soc.*, 2006, **128**, 11206–11210.

35 F. A. Cotton, G. Wilkinson, M. Bochmann and C. Murillo, *Advanced Inorganic Chemistry*, Wiley, 6th edn, 1998.

36 *Cambridge Structural Database, Version 5.35*, 2013.

37 T. N. Parac, D. L. Caulder and K. N. Raymond, *J. Am. Chem. Soc.*, 1998, **120**, 8003–8004.

38 C. R. K. Glasson, J. K. Clegg, J. C. McMurtie, G. V. Meehan, L. F. Lindoy, C. A. Motti, B. Moubaraki, K. S. Murray and J. D. Cashion, *Chem. Sci.*, 2011, **2**, 540–543.

39 M. Han, J. Hey, W. Kawamura, D. Stalke, M. Shionoya and G. H. Clever, *Inorg. Chem.*, 2012, **51**, 9574–9576.

40 I. A. Riddell, M. M. J. Smulders, J. K. Clegg, Y. R. Hristova, B. Breiner, J. D. Thoburn and J. R. Nitschke, *Nat. Chem.*, 2012, **4**, 751–756.

41 B. E. F. Tiedemann and K. N. Raymond, *Angew. Chem., Int. Ed.*, 2006, **45**, 83–86.

42 L. Trembleau and J. Rebek, *Science*, 2003, **301**, 1219–1220.

43 Y.-R. Zheng, K. Suntharalingam, T. C. Johnstone and S. J. Lippard, *Chem. Sci.*, 2015, **6**, 1189–1193.

44 F. A. Cotton and M. Goodgame, *J. Am. Chem. Soc.*, 1961, **83**, 1777–1780.

45 E. Shurdha, C. E. Moore, A. L. Rheingold, S. H. Lapidus, P. W. Stephens, A. M. Arif and J. S. Miller, *Inorg. Chem.*, 2013, **52**, 10583–10594.

46 J. R. Turkington, V. Cocalia, K. Kendall, C. A. Morrison, P. Richardson, T. Sassi, P. A. Tasker, P. J. Bailey and K. C. Sole, *Inorg. Chem.*, 2012, **51**, 12805–12819.

47 R. J. Ellis, J. Chartres, K. C. Sole, T. G. Simmance, C. C. Tong, F. J. White, M. Schroder and P. A. Tasker, *Chem. Commun.*, 2009, 583–585.

48 A. M. Wilson, P. J. Bailey, P. A. Tasker, J. R. Turkington, R. A. Grant and J. B. Love, *Chem. Soc. Rev.*, 2014, **43**, 123–134.

49 G. J. Kleywegt and T. A. Jones, *Acta Crystallogr., Sect. D: Biol. Crystallogr.*, 1994, **50**, 178–185.

50 J. K. Clegg, J. Cremers, A. J. Hogben, B. Breiner, M. M. J. Smulders, J. D. Thoburn and J. R. Nitschke, *Chem. Sci.*, 2013, **4**, 68–76.

51 P. A. Gale, *Chem. Soc. Rev.*, 2010, **39**, 3746–3771.

52 I. S. Tidmarsh, B. F. Taylor, M. J. Hardie, L. Russo, W. Clegg and M. D. Ward, *New J. Chem.*, 2009, **33**, 366–375.

53 R. Custelcean, J. Bosano, P. V. Bonnesen, V. Kertesz and B. P. Hay, *Angew. Chem., Int. Ed.*, 2009, **48**, 4025–4029.

